

Articles

Triplet-State Photoexcitation Dipole-Jump Relaxation Method To Observe Adsorption/Desorption Kinetics at a Reversed-Phase Silica/Solution Interface

Stephanie R. Shield and Joel M. Harris*

Department of Chemistry, University of Utah, 315 South 1400 East, Salt Lake City, Utah 84112-0850

Electronic excitation of a probe chromophore can lead to a change in dipole moment that influences its activity or solubility in solution and changes its relative affinity for partitioning between two phases. Photoexcitation of a probe molecule can, therefore, perturb a sorption equilibrium, and the relaxation kinetics of the probe to the new equilibrium conditions can be monitored in a time-resolved luminescence experiment. The adsorption/desorption kinetics of rose bengal, distributed between a C-18 derivatized porous-silica surface and a liquid mobile-phase solution, were investigated. These kinetics were determined by observing their effect on the phosphorescence decay of the triplet state of rose bengal and its quenching by ferricyanide. The methanol/water solvent compositions were varied to alter the fraction of adsorbed rose bengal. The adsorption rate constant for the triplet state was determined from the dependence of the phosphorescence relaxation rate on dye concentration in solution. The results indicate that the adsorption kinetics are diffusion controlled and that the relaxation is influenced by efficient triplet-energy transfer between excited- and ground-state rose bengal at the C-18 silica/solution interface.

Most of our understanding of chemistry at solid/liquid interfaces has been inferred from solute retention equilibria measured by chromatography, adsorption isotherms, or other steady-state experiments. The subtle nature of chemical interactions that play a role in interfacial phenomena cannot generally be identified by equilibrium measurements alone. Interfacial kinetic measurements can provide important information about rates of adsorption and desorption that govern adsorption equilibria.

Despite the importance of interfacial kinetics to the efficiency of chromatography and catalysis, or the time response of sensors, few techniques currently exist to probe fast chemical events at dielectric (nonconductive) interfaces. To measure the rate of an interfacial process, a fast perturbation to the equilibrium condition is required to alter the concentrations or activities of surface

species. Electrochemical perturbations are not feasible for insulating, dielectric surfaces; flow methods are limited by molecular diffusion through the stagnant solvent layer adjacent to a solid surface. To avoid the difficulty of imposing a fast concentration change at an interface, relaxation kinetics¹ can be employed whereby the activities of species in equilibrium are perturbed by a rapid change in conditions such as temperature, pressure, or electric field.² The equilibrium constant of a reversible reaction is thus shifted to a new value, and the rate of relaxation of the system to the new conditions is monitored to determine the reaction kinetics.

Several approaches to perturbing adsorption/desorption equilibria have been developed for studying the kinetics of reversed-phase chromatographic systems: a pressure-jump experiment utilizes the sensitivity of equilibrium to changes in pressure when there is a change in the molar volume upon adsorption.^{3,4} A temperature jump provided by either a Joule-discharge^{5–7} or laser⁸ heating of the sample can be used to perturb an adsorption/desorption equilibrium based on the temperature sensitivity of the equilibrium constant, which depends on the enthalpy of reaction. Total-internal-reflection fluorescence-correlation spectroscopy (TIR-FCS) has also been employed to measure adsorption/desorption kinetics at C-18 modified flat silica surfaces,⁹ where the relaxation to fluctuations in number of adsorbed molecules is measured. These relaxation techniques have revealed some detail about adsorption kinetics at reversed-phase chromatographic surfaces, but the conditions of the surface/solution chemistry must be altered in order to meet the needs of the experiment; these techniques require either extreme pressure

(1) Eigen, M. *Discuss. Faraday Soc.* **1954**, 17, 194–205.

(2) Bernasconi, C. F. *Relaxation Kinetics*; Academic Press: New York, 1976.

(3) Marshall, D. B.; Burns, J. W.; Conolly, D. E. *J. Chromatogr.* **1986**, 360, 13–24.

(4) Marshall, D. B.; Burns, J. W.; Conolly, D. E. *J. Am. Chem. Soc.* **1986**, 108, 1087–1088.

(5) Waite, S. W.; Marshall, D. B.; Harris, J. M. *Anal. Chem.* **1994**, 66, 2052–2061.

(6) Ren, F. Y.; Waite, S. W.; Harris, J. M. *Anal. Chem.* **1995**, 67, 3441–3447.

(7) Ren, F. Y.; Harris, J. M. *Anal. Chem.* **1996**, 68, 1651–1657.

(8) Waite, S. W.; Holzwarth, J. F.; Harris, J. M. *Anal. Chem.* **1995**, 67, 1390–1399.

(9) Hansen, R. L.; Harris, J. M. *Anal. Chem.* **1998**, 70, 4247–4256.

changes for pressure-jump, high-salt concentrations for Joule-discharge heating, dispersed colloids for laser heating, or flat surfaces for TIR-FCS, which are not encountered in chromatography practice.

An alternative method of perturbing an adsorption equilibrium, which does not impose changes to typical sample conditions, employs the change in dipole moment of an adsorbed probe molecule upon photoexcitation. Many chromophores exhibit different solubility properties in an excited electronic state compared to the ground state. For example, it has been reported that xanthone dye molecules dissolved in micelles exit the hydrophobic micellar core and enter the surrounding aqueous solution upon photoexcitation to the triplet state.^{10,11} A large change in the dipole moment between the ground-state singlet and excited triplet states accounted for the observed solubility differences. In addition, it was shown that halogenated fluorescein derivatives also display a similar hydrophobic-to-hydrophilic shift in solubility upon photoexcitation due to an increase in dipole moment in the excited state.^{12,13}

The application of organic dye molecules as biological or chemical probes is widespread. Luminescence from the excited state provides a convenient and sensitive method to monitor interfacial environments since the emission spectroscopy and decay kinetics are sensitive to environment.¹⁴ Phosphorescence from excited triplet probes is not as commonly employed as more strongly allowed fluorescence emission from excited singlet states; nevertheless, the slower decay rate of phosphorescence allows kinetics to be probed on longer time scales using triplet-state probes. For example, erythrosin (tetraiodofluorescein) has been a useful probe for monitoring slow (μ s to ms) rotational mobility of proteins and biomolecules.^{15–19} Rose bengal (tetrachlorotetraiodofluorescein) has been used as a probe in studying the structure of micelles; rose bengal associates with the hydrophobic core of the micelle, and the photophysics of the excited-state dye can be useful in characterizing the heterogeneous micellar environment.^{20–22} Time-resolved emission measurements have been used to determine the equilibrium constant for rose bengal dissolved within micelles as well as entry and exit rate constants.^{12,13,20,23} Although rose bengal is anionic, it can partition into negatively charged micelles when the electrostatic repulsion is reduced under high ionic strength conditions.²¹

In this work, rose bengal is employed to probe excited-state kinetics at a C-18 derivatized silica/solution interface. Adsorption/

desorption kinetics of rose bengal at the alkylated silica surface are monitored in the phosphorescence decay of its excited triplet state and its quenching by ferricyanide. The methanol/water solvent compositions are varied to alter the fraction of adsorbed rose bengal, as determined from chromatographic retention of the compound. The adsorption rate constant for the triplet state is determined from the decay rate of phosphorescence for various rose bengal concentrations. The desorption rate constant is estimated from the adsorption rate and the adsorption equilibrium constant.

EXPERIMENTAL SECTION

Instrumentation. A frequency tripled Quanta Ray model GCR-11 Nd:YAG laser ($\lambda_e = 355$ nm) was operated at 10 Hz and blocked by a shutter to provide a repetition rate of 1.0 Hz. The 5-ns UV (90–120 μ J) excitation pulse was weakly focused to a spot size of 2.2 mm and used to photoexcite the sample. The photon density was $\leq 2.5 \times 10^{15}$ photons/cm², and triplet–triplet annihilation was avoided as a significant contribution to the decay rate by keeping the excitation photon density less than $\sim 1 \times 10^{16}$ photons/cm².

Phosphorescence was collected at 90° from the excitation axis and filtered through a 1.0-cm path of a 0.5% aqueous solution of sodium nitrite and three glass filters, Schott KV408, KV550, and RG630; the long-wavelength pass band is determined by the last filter to be > 630 nm. The filtered emission was detected using a red-sensitive (to 800 nm) Hamamatsu R928 photomultiplier tube and digitized with a LeCroy 9450 oscilloscope. Fifty phosphorescence transients were averaged with an oscilloscope input termination resistance of 50 Ω .

Reagents and Solutions. Rose bengal (Sigma, 90%), potassium hexacyanoferrate(III), also known as ferricyanide (Fisher, Certified ACS), potassium chloride (Mallinckrodt, AR), methanol (Fisher, Optima), and water (Fisher, HPLC grade) were used as received. The C-18 derivatized porous silica gel was EM Science LiChrosorb RP-18 with a 10- μ m particle diameter, a 100-Å pore diameter, and a 9.5% carbon loading of monomeric C-18 ligands (not end capped). Silica suspensions of 10 mg/mL were used in all experiments. Oxygen was removed from the suspensions and the free solution samples by three freeze–pump–thaw cycles pumped to a submilliTorr base pressure.

A constant ionic strength of 50 mM was maintained in all solutions using KCl. A 100 μ M stock solution of rose bengal and a 1 mM stock solution of ferricyanide were prepared (and sonicated) in the various solvent compositions with KCl present and were used immediately. The concentration of rose bengal for all experiments was 4–5 μ M. For free-solution quenching experiments, the ferricyanide concentrations were 0, 10, 20, and 30 μ M; for studies of heterogeneous quenching in the presence of C-18 silica, ferricyanide concentrations were 0, 20, 50, and 80 μ M. The fraction of rose bengal adsorbed to the C-18 silica was determined from chromatographic retention measurements and controlled by varying the methanol/water solution composition. All silica suspensions were sonicated for 2 min to remove trapped air from within the pores. Following deoxygenation (see above), the silica was allowed to settle for 15 min into a 2-mm-i.d. Suprasil quartz capillary tube attached to the freeze–pump–thaw cell. This step provided a gravity-packed silica bed, which increased the sensitivity for observing chemistry at the C-18 interface and assured a

- (10) Abuin, E. B.; Scaiano, J. C. *J. Am. Chem. Soc.* **1984**, *106*, 6274–6283.
- (11) Scaiano, J. C.; Paraskevopoulos, C. I. *Can. J. Chem.* **1984**, *62*, 2351–2354.
- (12) Seret, A.; Van de Vorst, A. *J. Phys. Chem.* **1990**, *94*, 5293–5299.
- (13) Seret, A.; Van de Vorst, A. *J. Photochem. Photobiol. A: Chem.* **1988**, *43*, 193–206.
- (14) Rutan, S. C.; Harris, J. M. *J. Chromatogr., A* **1993**, *656*, 197–215.
- (15) Bowers, P. G.; Porter, G. *Proc. R. Soc. London Ser. A* **1967**, *299*, 348–353.
- (16) Garland, P. B.; Moore, C. H. *Biochem. J.* **1979**, *183*, 561–572.
- (17) Jovin, T. M.; Bartholdi, M.; Vaz, W. L. C.; Austin, R. H. *Ann. N.Y. Acad. Sci.* **1981**, *366*, 176–196.
- (18) Corin, A. F.; Blatt, E.; Jovin, T. M. *Biochemistry* **1987**, *26*, 2207–2217.
- (19) Tilley, L.; Sawyer, W. H.; Morrison, J. R.; Fidge, N. H. *J. Biol. Chem.* **1988**, *263*, 17541–17547.
- (20) Reed, W.; Politi, M. J.; Fendler, J. H. *J. Am. Chem. Soc.* **1981**, *103*, 4591–4593.
- (21) Rodgers, M. A. J. *J. Phys. Chem.* **1981**, *85*, 3372–3374.
- (22) Hoebeke, M.; Gandin, E.; Decuyper, J.; Van de Vorst, A. *J. Photochemistry* **1986**, *35*, 245–250.
- (23) Bryukhanov, V. V.; Laurinas, V. G.; Levshin, L. V.; Sokolova, L. K. *Appl. Spectrosc.* **1990**, *52*, 386–391.

high concentration of surface sites comparable to chromatographic conditions.

Chromatographic Measurements. Chromatographic retention measurements were performed on an HPLC system consisting of an Isco model 2350 pump and an Isco model 229 UV/visible absorbance detector operated at 254 nm. A reversed-phase C-18 chromatographic column (4.6 mm i.d. \times 150 mm), packed with the same 10- μ m LiChrosorb RP-18 used in the spectroscopy experiments, was purchased from Phenomenex (Torrance, CA). The amount of silica in the packed column was reported by Phenomenex to be \sim 2.0 g. The volume of the mobile phase was determined from the elution time of unretained species, D₂O, or phloroglucinol and found to be 1.63 mL. The mass of silica, the volume of the mobile phase, and the pore volume (1.25 mL/g) were used to estimate the adsorption equilibrium constant. Chromatographic capacity factors for rose bengal were determined at various methanol/water compositions in order to control the amount of dye adsorbed to the surface.

Data Analysis. A single-exponential decay model, weighted for photon shot noise, was used to fit the free-solution time-resolved phosphorescence decay of rose bengal. The observed free-solution lifetimes were used in a Stern–Volmer analysis to calculate a rate constant for quenching by ferricyanide. Time-resolved transients from triplet-state rose bengal adsorbed to C-18 porous silica were fit to a two-exponential decay model. This two-component model is needed to describe the observed kinetic processes: the fast relaxation of the adsorption equilibrium to the change in dipole moment and the slower, average decay of adsorbed and free-solution excited triplet states (see below). The kinetic models were compiled in Microsoft Fortran and utilized a Marquardt algorithm to minimize χ^2 and optimize the kinetic parameters and the population amplitudes. Phosphorescence transients were acquired in triplicate in order to estimate uncertainties of the decay rates and the quenching rates derived from the Stern–Volmer analysis. The plotted error bars are ± 1 standard deviation, and the uncertainties in the rate constants are reported at ± 2 standard deviations.

RESULTS AND DISCUSSION

Adsorption of Rose Bengal on C-18 Silica. To characterize the adsorption equilibrium of rose bengal, chromatographic retention times were measured on C-18 silica. From the elution time of the unretained species (t_0) and the retention time of rose bengal (t_r), the capacity factor was calculated, $K' = (t_r - t_0)/t_0$. The capacity factor, K' , is a ratio of the moles of solute in the stationary phase to the moles of solute in the mobile phase. The fraction of adsorbed rose bengal is then predicted to be $K'/(1 + K')$.

In the chromatographic retention measurements of rose bengal on C-18 silica, it was found that the addition of electrolyte to the mobile phase significantly influenced adsorption of the dye (the dye structure is illustrated in Figure 1). As shown in Table 1, little or no retention is observed in the absence of electrolyte. Upon the addition of 10 mM KCl, however, the retention of the dye on the C-18 surface becomes significant (see Table 1). Under 65/35 methanol/water conditions, K' increased from no detectable retention ($K' < 0.02$) in the absence of electrolyte to $K' = 9.28$ in 10 mM KCl. The retention further increased with higher concentrations of KCl and showed a $K' = 15.7$ at 50 mM KCl. This

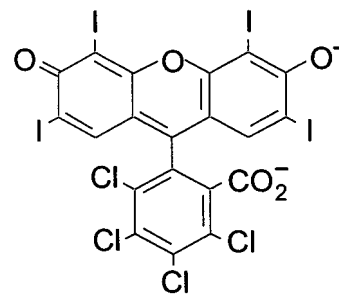


Figure 1. Structure of rose bengal.

Table 1. Chromatographic Retention of Rose Bengal on C-18 Silica versus Mobile-Phase Composition

methanol/water (v/v)	[KCl] (mM)	K'
80/20	0	<0.02
	20	1.15
	50	1.60
65/35	0	<0.02
	10	9.28
	20	11.7
	50	15.7
50/50	0	0.14
	50	214
45/55	50	630

increase in K' with the addition of electrolyte was evident under various solvent compositions as seen from Table 1. The results are similar to those of Abuin and Scaiano,¹⁰ who reported more favorable binding of a negatively charged probe to the hydrophobic core of negatively charged micelles upon addition of electrolyte.

The inhibition of rose bengal retention on the C-18 silica surface arises from the residual negative charge from unreacted silanol groups on the surface. The C-18 ligands even at the highest coverages react with only half the silanol groups on the silica surface;²⁴ the residual silanol groups deprotonate at pH ≥ 2.5 and generate a negatively charged surface in the presence of water. In the absence of electrolyte, electrostatic repulsion prevents adsorption of the anionic dye. The double layer thickness can be estimated from the Debye length (κ^{-1}):²⁵

$$\kappa = \left(\frac{\sum_i \rho_{\infty,i} e^2 z_i^2}{\epsilon \epsilon_0 k T} \right)^{1/2} \quad (1)$$

where $\rho_{\infty,i}$ is the total concentration of ions in the bulk solution, e is the elementary charge, and z_i is the magnitude of the charge on the ions. A 10 mg/mL suspension in 45/55 and 65/35 methanol/water has a pH of 6. Based on the concentration of ions in solution determined from the pH, the double-layer thickness, κ^{-1} , for this solution is estimated to be ≥ 360 nm. This distance is much larger than the pore diameter and does not allow dye interaction with the hydrophobic C-18 chains; therefore, no

(24) Iler, R. K. *The Chemistry of Silica, Solubility, Polymerization, Colloid and Surface Properties and Biochemistry*; John Wiley & Sons: New York, 1979.

(25) Israelachvili, J. N. *Intermolecular & Surface Forces*, 2nd ed.; Academic: London, 1992; Chapter 12.

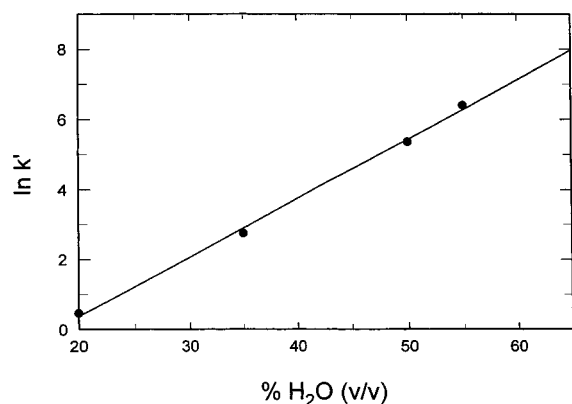


Figure 2. Log of the capacity factor, K' , for chromatographic retention rose bengal on a C-18 silica column versus volume percent water in the methanol/water mobile phase.

adsorption is observed. By adding 50 mM KCl, however, the double-layer thickness decreases to 1.4 nm in water, which provides an upper bound for κ^{-1} in mixed solvents. The dielectric constant of methanol/water is less than pure water, and thus, the double-layer thickness would be slightly smaller. The Debye length of 1.4 nm is much less than the pore diameter (10 nm) and comparable to the C-18 chain length. Under these conditions, the double layer is compressed and screening of the surface potential by the electrolyte allows hydrophobic interactions between rose bengal and the C-18 ligands to overcome the electrostatic repulsion between the negatively charged dye and the negatively charged silica surface. With 50 mM KCl in the mobile phase, hydrophobic interactions govern solute retention as is evident in the large increase in the capacity factor with increasing volume fraction of water in the mobile phase as shown in Figure 2. This plot of $\log(K')$ versus volume fraction water is linear, $r^2 = 0.997$, as expected for reversed-phase retention.²⁶

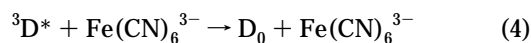
Phosphorescence Decay Kinetics of Rose Bengal. The triplet state of the dye is populated by photoexcitation ($h\nu$) of the ground-state and subsequent intersystem crossing of the excited-singlet state:



The excited triplet state of the dye decays back to the ground state, with a fraction of the excited molecules emitting phosphorescence, $h\nu'$:



In the presence of ferricyanide quencher, $\text{Fe}(\text{CN})_6^{3-}$, the triplet state undergoes quenching through an electron-transfer intermediate:²⁷



Phosphorescence is collected for various quencher concentrations, and the observed decay rates are used to determine the quenching rate constant using a Stern–Volmer analysis.

The hydrophobic nature of aromatic rings in rose bengal allows for a strong association with the C-18 chains to avoid contact with the aqueous solution. The adsorbed and free solution dye are in equilibrium:

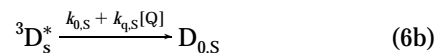


where $D_{0,\text{FS}}$ represents the ground state of free-solution rose bengal in equilibrium with $D_{0,\text{S}}$, dye adsorbed to the surface of the C-18 silica. The concentration of accessible surface sites in the silica material is represented by S . The adsorption rate constant is k_{ads} , and the rate constant for desorption is k_{des} .

It has been shown in micellar studies that the excited-triplet state of rose bengal is more polar than the ground state, which drives a transfer of a fraction of the excited population from the hydrophobic micellar core into solution.^{10,12,13} A perturbation to the equilibrium occurs upon excitation, following which the system reestablishes the equilibrium between the adsorbed (${}^3D_{\text{S}}^*$) and free solution (${}^3D_{\text{FS}}^*$) populations of the excited dye:



The adsorption rate constant for the triplet state is k_{ads}^* and the desorption rate constant is k_{des}^* . The asterisk is used to distinguish these rates from the adsorption/desorption rates of the ground-state dye molecule, as they differ in response to the change in dipole moment upon photoexcitation. The populations of adsorbed and free-solution excited states decay according to



It is expected that two different quenching rate constants will be distinguished for solution-phase ($k_{\text{q,FS}}$) and the surface-bound ($k_{\text{q,S}}$) triplet states since adsorption and partitioning of the dye on the C-18 surface can reduce the frequency of encounter with solution-phase quenchers.^{28–29} The solvent composition was varied in order to vary the adsorption/desorption kinetics and determine the rate constants.

Decay Kinetics and Quenching of Triplet Rose Bengal.

The free-solution phosphorescence decay of triplet rose bengal followed single-exponential decay kinetics as expected, where the unquenched lifetime was 130 μs corresponding to a decay rate, $k_{0,\text{FS}} = 7.7 \times 10^3 \text{ s}^{-1}$. Under 65/35 methanol/water conditions ($K' = 15.7$), the time-resolved phosphorescence of adsorbed triplet rose bengal also followed first-order decay kinetics with a 70- μs unquenched lifetime or a decay rate, $k_{0,\text{S}} = 1.4 \times 10^4 \text{ s}^{-1}$. The phosphorescence decay rate of adsorbed rose bengal was measured versus the solution concentration of ferricyanide (0, 20, 50,

(26) Karger, B. L.; Gant, J. R.; Hartkopf, A.; Weiner, P. *J. Chromatogr.* **1976**, *128*, 65–78.

(27) Kasche, V.; Lindqvist, L. *Photochem. Photobiol.* **1965**, *4*, 932–933.

(28) Carr, J. W.; Harris, J. M. *Anal. Chem.* **1987**, *59*, 2546–2550.

(29) Wong, A. L.; Hunnicutt, M. L.; Harris, J. M. *Anal. Chem.* **1991**, *63*, 1076–1081.

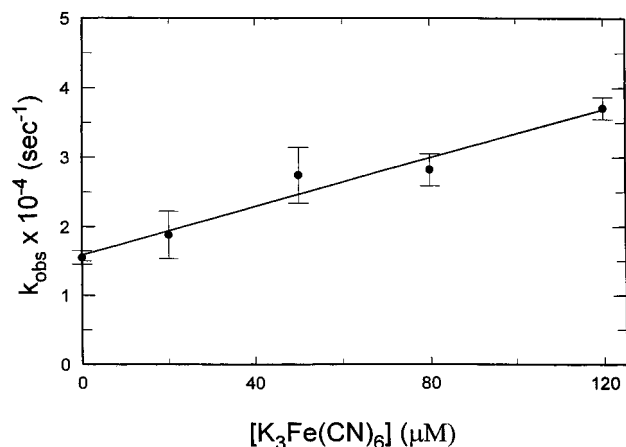


Figure 3. Determination of the rate constant for quenching triplet rose bengal at a C-18 silica surface by ferricyanide in 65/35 methanol/water. The rose bengal concentration was 5 μM , and the ferricyanide concentrations were 0, 20, 50, 80, and 120 μM . The quenching rate constant was determined from the slope to be $k_q = (1.8 \pm 0.4) \times 10^8 \text{ M}^{-1} \text{ s}^{-1}$. The unquenched triplet lifetime on the surface was 70 μs .

80, and 120 μM). The decay rates were plotted versus quencher concentration, and the slope of the resulting Stern–Volmer plot shown in Figure 3 is the interfacial quenching rate constant, $k_{q,s} = (1.8 \pm 0.4) \times 10^8 \text{ M}^{-1} \text{ s}^{-1}$. The free-solution rate constant for quenching rose bengal was determined in the same manner for ferricyanide concentrations of 0, 10, 20, 30, and 40 μM ; a Stern–Volmer analysis was used to determine the quenching rate constant, $k_{q,FS} = (5.8 \pm 0.3) \times 10^8 \text{ M}^{-1} \text{ s}^{-1}$. The surface quenching rate constant is smaller than the corresponding free-solution value by a factor of 3.2. This reduction in the rate of surface quenching compared to free solution was previously observed for fluorescence quenching of probes adsorbed on C-18 surfaces;^{28,29} this rate reduction arises from several factors: restricted motion of one reactant by immobilization on the surface,³⁰ excluded solution volume around that reactant,^{31,32} and protection from encounter by free-solution species by the C-18 ligands.^{28,29}

Since the phosphorescence transients for surface-adsorbed rose bengal fit a first-order decay model, it appears that relaxation of the adsorption/desorption equilibrium to the change in dipole of the probe upon excitation is too fast to be observed. Based on the adsorbed fraction of molecules, $\sim 6\%$ of the initial excited-state population is present in free solution and should have different decay rates and quenching kinetics. The fraction of longer-lived free-solution excited states ($\tau_{0,FS} = 130 \mu\text{s}$) should be distinguishable from the shorter-lived surface-bound triplet states ($\tau_{0,s} = 70 \mu\text{s}$). If the rate at which the excited-state population adsorbs and desorbs from the surface is fast relative to the decay rates of the excited states, however, then the observed decay rate is a population-weighted average, dominated by the larger surface-bound fraction.

Under solvent conditions with greater than 50% water, the phosphorescence decay of rose bengal adsorbed to the C-18 silica was *no longer* single exponential, but rather followed a bi-exponential decay model with one positive and one negative

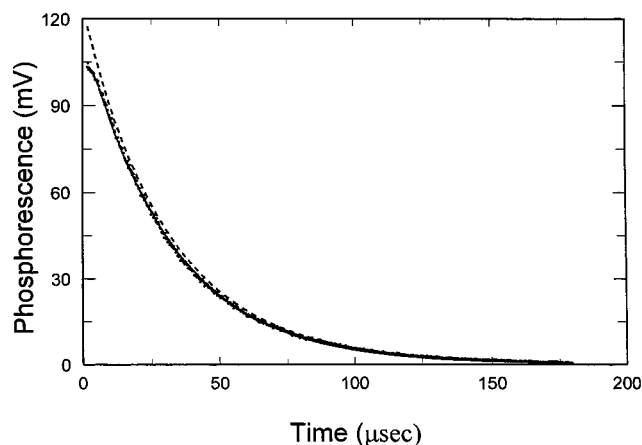


Figure 4. Time-resolved phosphorescence emission transient for an unquenched rose bengal suspension with C-18 silica in 45/55 methanol/water. The rose bengal concentration was 10 μM , and the silica concentration was 10 mg/mL. The dashed line shows the two-exponential decay fit where the amplitudes for both components were positive. The solid line is a two-exponential decay fit with one positive and one negative preexponential.

preexponential factor. This rise in emission was not observed for lower water content solvent conditions. Figure 4 shows a time-resolved phosphorescence emission transient for unquenched rose bengal in a C-18 silica suspension in 45/55 methanol/water solution. The dashed line shows the two-exponential decay fit where the amplitudes for both components were positive. It can be seen that this fit significantly overestimates the initial phosphorescence intensity. The dotted line is a two-exponential fit with one with a positive preexponential, corresponding to a slow decay of the phosphorescence, and one negative preexponential, corresponding to a fast early rise in the signal; this model fits the data even at early times.

The small, rapid rise at the beginning of the emission transients appears to be a relaxation of the rose bengal population to a new adsorption equilibrium condition. This rise is only seen at early times because this relaxation is fast compared to the slow decay of the excited population. The *sign of the preexponential is consistent* with the quantum yield for emission in solution being greater than that on the surface, which is supported by the difference in the unquenched phosphorescence decay rate of the dye between the two environments. The second-exponential component with a positive preexponential describes the decay of triplet populations (on the surface and in solution) that are not distinguishable because the adsorption/desorption kinetics (eq 6a) are fast compared to the decay rate of the excited state (eqs 6b and 6c). Again, if the adsorbed and free-solution excited-state populations exchange on a time scale that is fast compared to their decay, then a population-weighted average of the excited-state decay rates is observed. The magnitude of the rate constant is consistent with its assignment as the average decay of the excited-state population.

Figure 5 shows the phosphorescence decay from triplet rose bengal for ferricyanide concentrations of 0, 20, 50, 80, and 120 μM (from top to bottom) along with the best fit to a two-exponential decay model with one positive and one negative amplitude. The Stern–Volmer plot of the observed rates for both components versus quencher concentration is shown in Figure 6. The positive amplitude component describing the population

(30) Astumian, R. D.; Schelly, Z. A. *J. Am. Chem. Soc.* **1984**, *106*, 304–308.

(31) Wong, A. L.; Hunnicutt, M. L.; Harris, J. M. *J. Phys. Chem.* **1991**, *95*, 4489–4495.

(32) Kavanagh, R. J.; Thomas, J. K. *Langmuir* **1998**, *14*, 352–362.

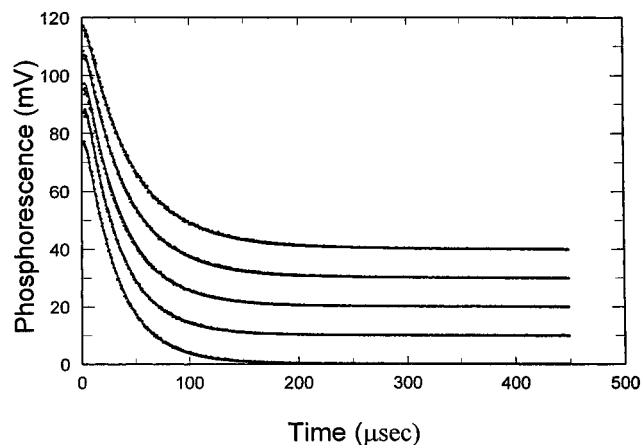


Figure 5. Phosphorescence decay for triplet rose bengal quenched by ferricyanide with the best fit to the two-exponential decay with one positive and one negative amplitude in 45/55 methanol/water. The ferricyanide concentrations were 0, 20, 50, 80, and 120 μM (from top to bottom). The transients are scaled and offset by increments of 10 mV.

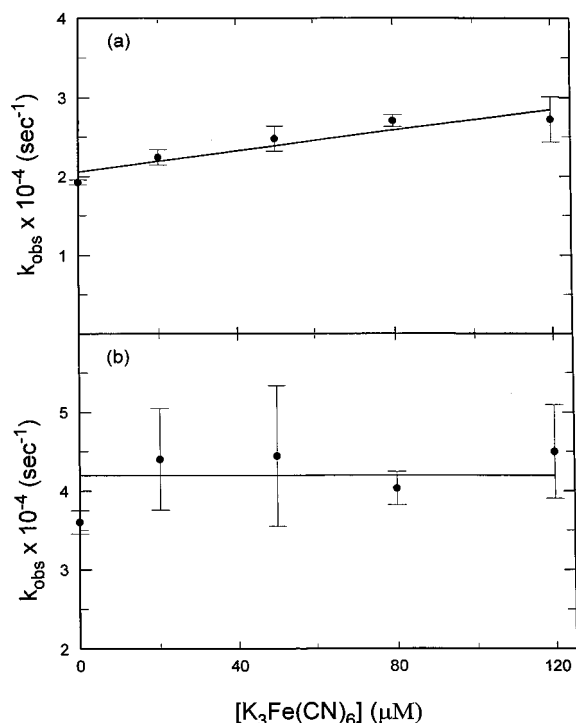


Figure 6. Stern–Volmer plot of the decay rates versus ferricyanide concentration for rose bengal/C-18 silica suspensions in 45/55 methanol/water. (a) The decay rate of the positive preexponential component depended on quencher concentration with a quenching rate constant determined from the slope was $k_q = (8.7 \pm 1.2) \times 10^7 \text{ M}^{-1} \text{ s}^{-1}$. (b) The rise of the negative preexponential component did not depend on quencher concentration and had an average rate of $k_{\text{neg}} = (4.2 \pm 0.5) \times 10^5 \text{ s}^{-1}$.

decay kinetics (Figure 6a) shows a linear dependence of the decay rate on quencher concentration. The rate constant for quenching is determined from the slope to be $k_{q,s} = (8.7 \pm 1.2) \times 10^7 \text{ M}^{-1} \text{ s}^{-1}$. The negative amplitude component (Figure 6b) has an average rate constant of $k_{\text{neg}} = (4.2 \pm 0.6) \times 10^5 \text{ s}^{-1}$, but does *not* show a dependence on the quencher concentration.

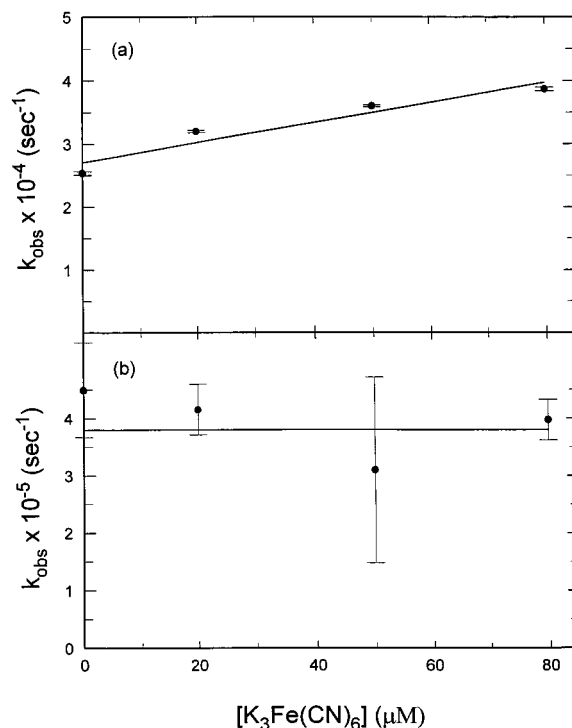


Figure 7. Stern–Volmer plot of the observed decay rates versus ferricyanide concentration at 35/65 methanol/water. (a) The longer-lived component was quenched by ferricyanide with a quenching rate constant determined from the slope to be $k_q = (1.6 \pm 0.3) \times 10^8 \text{ M}^{-1} \text{ s}^{-1}$. (b) The faster (negative preexponential) component did not vary with ferricyanide concentration and exhibited an average rate of $k_{\text{neg}} = (3.8 \pm 1.2) \times 10^5 \text{ s}^{-1}$.

Phosphorescence quenching of free-solution rose bengal was determined for various ferricyanide concentrations under the 45/55 methanol/water conditions. A Stern–Volmer analysis of the observed decay rate for 4 μM free-solution rose bengal quenched by ferricyanide at concentrations of 0, 10, 20, and 30 μM found the free-solution quenching rate constant to be $k_{q,\text{FS}} = (6.5 \pm 0.7) \times 10^8 \text{ M}^{-1} \text{ s}^{-1}$, which was a factor of 7.5 times larger than the adsorbed dye quenching rate constant. The reduction in the rate constant by this magnitude is again reasonable, given that one reactant is adsorbed to a surface that reduces the rate of encounter between the excited state and the solution-phase quencher. Therefore, it is postulated that the positive amplitude component describes decay of primarily adsorbed triplet rose bengal, which is quenched by ferricyanide. The quenching rate constant determined from the observed decay rates represents an average of the quenching occurring on the surface and in solution.

Under 35/65 methanol/water conditions, the adsorption of rose bengal is very high, too large to be measured directly using chromatography. A plot of $\ln K$ versus percent H_2O is linear (see Figure 2), which provides a relationship that can be extrapolated to predict K for higher water conditions.³³ From this plot, it was estimated that $K = 2900$ for 35/65 methanol/water. The phosphorescence emission from triplet rose bengal followed a two-exponential decay model with one positive and one negative amplitude. Figure 7 shows the Stern–Volmer analysis of the observed rates versus ferricyanide concentration for components

(33) Carr, J. W.; Harris, J. M. *Anal. Chem.* **1988**, *60*, 698–702.

Table 2. Rates of Rose Bengal Phosphorescence Quenching and Decay

	65/35 methanol/water	45/55 methanol/water	35/65 methanol/water
quenching ^a rate in free solution, $k_{q,FS}$ ($M^{-1} s^{-1}$)	$(5.8 \pm 0.3) \times 10^8$	$(6.5 \pm 0.7) \times 10^8$	$(7.2 \pm 0.5) \times 10^8$
unquenched decay rate in free solution, $k_{0,FS}$ (s^{-1})	$(7.7 \pm 0.5) \times 10^3$	$(6.3 \pm 0.5) \times 10^3$	$(7.7 \pm 0.5) \times 10^3$
quenching ^a rate on C-18 silica, k_q ($M^{-1} s^{-1}$)	$(1.8 \pm 0.4) \times 10^8$	$(8.7 \pm 1.2) \times 10^7$	$(1.6 \pm 0.3) \times 10^8$
unquenched decay rate on C-18 silica, $k_{0,S}$ (s^{-1})	$(1.5 \pm 0.2) \times 10^4$	$(1.9 \pm 0.2) \times 10^4$	$(2.5 \pm 0.3) \times 10^4$
adsorption relaxation rate on C-18 silica, k_{neg} (s^{-1})		$(4.2 \pm 0.5) \times 10^5$	$(3.8 \pm 1.2) \times 10^5$

^a Quenching by potassium ferricyanide.

in 35/65 methanol/water. The longer-lived decay component was quenched by ferricyanide with a quenching rate constant determined from the slope (Figure 7a) to be $k_{q,S} = (1.6 \pm 0.3) \times 10^8 M^{-1} s^{-1}$. The decay rate of the shorter-lived negative preexponential component, $k_{neg} = (3.6 \pm 1.6) \times 10^5 s^{-1}$, was again not dependent on quencher concentration (Figure 7b). The free-solution rate constant was determined under these solvent conditions and found to be $k_{q,FS} = (7.2 \pm 0.5) \times 10^8 M^{-1} s^{-1}$. The rate constant for quenching was reduced by a factor of 4.5 for rose bengal on the C-18 silica surface compared to free solution.

Under the stronger adsorption conditions, a change in the surface population (from the perturbation of the adsorption equilibrium) makes a *larger change* in the concentration of excited states in solution where the luminescence yield is higher, so that the relaxation of the adsorption equilibrium produces a greater change in signal amplitude. The ratio of the negative and the positive preexponential factors for unquenched rose bengal was 0.1 for 45/55 methanol/water ($K = 630$) where 6% of the dye is in the solution phase. This ratio increases to 0.4 in 35/65 methanol/water ($K = 2900$) where <1% of the initial dye population is in free solution, further supporting the assignment of the negative preexponential to adsorption/desorption relaxation. The quenching rate constants, unquenched decay rates, and relaxation rates for the negative preexponential component are summarized in Table 2 for free-solution and C-18 silica experiments in the various solvent compositions. The free-solution and surface quenching rates do not show a systematic or strong dependence on solvent composition. There is a noticeable trend in the unquenched excited-state decay rate of the probe on C-18 silica where the rate increases at higher fractions of water in solution; since this rate represents an average of the excited-state decay of surface and solution populations (see above), its increase is consistent with a greater fraction of probe on the surface where the decay is more rapid.

Adsorption/Desorption Kinetics. In the above analysis, we postulate that the negative amplitude component describes the relaxation of the excited population to the new equilibrium condition in eq 6a. Since the rate of this relaxation process is much faster than the decay of the excited population, then the coupling of the two rate processes can be neglected and the kinetics behavior on the two time scales can be analyzed independently.² The relaxation of the adsorption/desorption equilibrium at early times is analyzed as follows: since the concentration of surface sites within the porous particles is much higher than the excited-state concentration, then pseudo-first-order conditions for the adsorption kinetics are met. From the excited-state equilibrium given in eq 6a, the final concentration of the triplet-state species

can be described with respect to the initial concentration after perturbation of the equilibrium:

$$[{}^3D_{FS}^*]_f = [{}^3D_{FS}^*]_i + x \quad (7a)$$

$$[{}^3D_S^*]_f = [{}^3D_S^*]_i - x \quad (7b)$$

where x represents the change in concentrations in response to the perturbation of the adsorption equilibrium. The general rate equation for the relaxation is given by

$$\frac{d[{}^3D_{FS}^*]}{dt} = \frac{-d[{}^3D_S^*]}{dt} = \frac{d([{}^3D_{FS}^*]_i + x)}{dt} = \frac{-d([{}^3D_S^*]_i - x)}{dt} = \frac{dx}{dt} \quad (8)$$

After substitution with the individual rate expressions, the rate equation can be simplified to

$$dx/dt = -\{k_{ads}([{}^3D_{FS}^*]_f + [S]) + k_{des}^*\}x - k_{ads}^*(x)^2 \quad (9)$$

Since the concentration of surface sites is in excess, and the relative perturbation of the populations and rates upon excitation is small (as shown by the relaxation amplitudes above), the term that is quadratic in x can be neglected. The observed relaxation rate is single exponential² with $dx/dt = -k_{ads}^*x$, where the observed rate is given by^{2,8}

$$k_{obs} = k_{ads}^*([{}^3D_{FS}^*] + [S]) + k_{des}^* \quad (10)$$

This observed rate is assigned to the early rise in the emission, due to the higher phosphorescence yield in solution and is represented by a negative preexponential amplitude (see above). By varying the concentration of dye in free solution, D_{FS} , and thus, the excited-state concentrations, the adsorption rate constant can be determined. Figure 8 shows the plot of the observed relaxation rate in 45/55 methanol/water versus rose bengal concentrations of 1, 4, and 10 μM on the lower x -axis, and excited triplet-state rose bengal concentrations determined from the excitation fluence to be 0.03, 0.11, and 0.28 μM are plotted on the upper x -axis.

The relaxation rate responds linearly to changes in the rose bengal concentration as predicted by eq 10. Using the triplet-state concentration and the slope of Figure 8, however, the adsorption rate constant is $(1.3 \pm 0.6) \times 10^{12} M^{-1} s^{-1}$, which is unrealistically

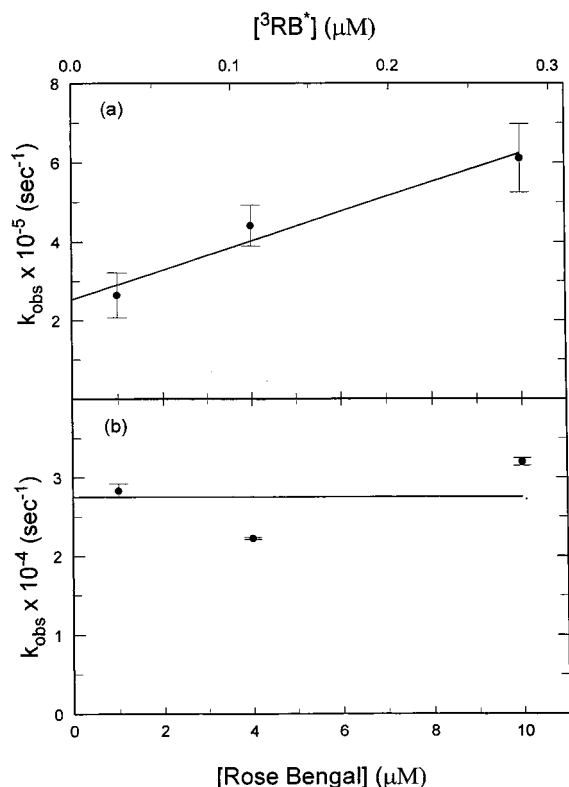


Figure 8. Determination of the adsorption rate constant for rose bengal at a C-18 silica surface in 45/55 methanol/water. The observed relaxation rate is plotted versus rose bengal ground-state concentrations on the lower x-axis and excited-state concentrations on the upper x-axis. (a) The C-18 silica adsorption rate constant for triplet rose bengal is determined from the slope from the rate of the negative amplitude component versus ground-state concentration to be $k_{\text{ads}} = (3.7 \pm 1.5) \times 10^{10} \text{ M}^{-1} \text{ s}^{-1}$. (b) The positive preexponential component does not vary with rose bengal concentration.

large, nearly 2 orders faster than diffusion-controlled. If the relaxation rate depends on the ground-state concentration, however, the adsorption rate constant is $k_{\text{ads}} = (3.7 \pm 1.5) \times 10^{10} \text{ M}^{-1} \text{ s}^{-1}$, which is on the order of a diffusion-controlled rate constant. A mechanism by which collisions between *ground-state rose bengal* and the surface can be controlling the excited-state equilibrium relaxation is energy exchange³⁴ between surface-adsorbed excited states and ground states of rose bengal. Few experiments are sensitive to homolytic triplet energy transfer.³⁴ Lechtken and Turro³⁵ measured the homolytic triplet energy transfer of acetone via a chemiexcitation technique and found the rate of triplet energy migration to be $3 \times 10^6 \text{ M}^{-1} \text{ s}^{-1}$. The isoenergetic triplet–triplet energy transfer rate from biacetyl to a series of compounds was reported to be $-1.6 \times 10^8 \text{ M}^{-1} \text{ s}^{-1}$,³⁶ and the reverse rate of triplet energy transfer from biphenyl to benzophenone (energetically uphill by 2 kcal/mol) was found to be $(1.6 \pm 0.8) \times 10^8 \text{ M}^{-1} \text{ s}^{-1}$.³⁷ These rates imply that homolytic triplet energy transfer can be as high as several percent of the diffusion-controlled limit.

(34) Turro, N. J. *Modern Molecular Photochemistry*; Benjamin/Cummings Publishing: Menlo Park, CA, 1978; Chapter 9.

(35) Lechtken, P.; Turro, N. J. *Angew. Chem., Int. Ed. Engl.* **1973**, *12*, 314.

(36) Birks, J. B. *Photophysics of Aromatic Molecules*; Wiley & Sons: New York, 1970.

(37) Poston, P. E.; Harris, J. M. *J. Photochem. Photobiol. A: Chem.* **1991**, *60*, 51–61.

Collisions between adsorbed triplet states and ground states of rose bengal on the C-18 surface should be frequent, on the order of 10^8 s^{-1} , due to the high surface concentration of the dye and the relatively fast lateral diffusion rates for charged adsorbates.³⁸ Therefore, triplet energy exchange could readily occur on a submicrosecond time scale, which would be consistent with the observed results. We conclude that triplet energy transfer accounts for the ground-state concentration dependence of the relaxation, and the ground-state adsorption rate constant is diffusion-controlled based on the dependence of the relaxation rate on the rose bengal concentration in solution.

The diffusion-controlled rate for rose bengal adsorption is ~ 1 order of magnitude faster than previously observed for a hydrophobic anionic probe molecule, anilidonaphthalenesulfonate (ANS), on alkylated silica surfaces^{5–7} under similar mobile-phase conditions and is comparable to the diffusion-controlled adsorption rate observed for a neutral probe, *N*-phenyl-1-naphthylamine (1-NPN). The slower adsorption rate for ANS was originally ascribed to rearrangement of the solvation cage around the sulfonate anion. While rose bengal is also anionic, the carboxylate and phenoxy anionic sites can distribute their electron density into the π -system of the molecule, which would result in less structuring of the methanol/water solvent around the solution-phase probe compared to the sulfonate group in ANS. The adsorption of rose bengal to the hydrophobic interface, therefore, exhibits a smaller energy barrier, comparable to the uncharged probe, 1-NPN.

Based on the adsorption rate measurement for rose bengal, an estimate of the desorption rate constant can be obtained from the intercept of the plot of k_{obs} versus $[D_{\text{FS}}]$:

$$k_{\text{obs},[D]=0} = k_{\text{ads}}[S] + k_{\text{des}} \quad (11)$$

The local concentration of surface sites, $[S]$, influences the collision rate with the surface and, thus, governs the adsorption rate contribution to the observed relaxation rates. The concentration of surface sites that govern adsorption kinetics is not well-defined in porous silica due to the complex pore geometry.²⁴ If the equilibrium ratio of adsorbed solute to free-solution solute is known, however, the desorption rate constant can be estimated without knowledge of $[S]$. At equilibrium, the concentration ratio of the adsorbed to free-solution dye is equal to the ratio of the adsorption and desorption rates:

$$[D_{\text{ads}}]/[D_{\text{FS}}] = k_{\text{ads}}[S]/k_{\text{des}} \quad (12)$$

Solving for $[S]$ and substituting into eq 11, the desorption rate constant is found to be

$$k_{\text{des}} = \frac{k_{\text{obs},[D]=0}}{1 + [D_{\text{ads}}]/[D_{\text{FS}}]} \quad (13)$$

The equilibrium concentration ratio, $[D_{\text{ads}}]/[D_{\text{FS}}]$, is equal to the mole ratio, $n_{\text{ads}}/n_{\text{FS}}$, since both concentrations are relative to the intraparticle solution volume. The mole ratio, $n_{\text{ads}}/n_{\text{FS}}$, is not identical to the measured chromatographic capacity factor, K' ,

(38) Zulli, S. L.; Kovaleski, J. M.; Zhu, X. R.; Harris, J. M.; Wirth, M. J. *Anal. Chem.* **1994**, *66*, 1708–1712.

since the latter includes molecules in the interparticle solution volume that do not participate in the relaxation kinetics on a 100- μ s time scale (diffusion over distances comparable to the silica particle diameter requires ~ 10 ms). To determine $n_{\text{ads}}/n_{\text{FS}}$ for the particle interior, one can correct K to include only the interparticle solvent volume:

$$n_{\text{ads}}/n_{\text{FS}} = K V_0/V_p m_p \quad (14)$$

where V_0 is the total solvent volume in the column, V_p is the specific pore volume of the silica, and m_p is the mass of the silica packed in the column. Under the 45/55 methanol/water condition, the chromatographic capacity factor, K , is 630 for rose bengal. Correcting this value for the smaller interparticle solution volume, gives $n_{\text{ads}}/n_{\text{FS}} \cong 1100$. From this value and k_{obs} extrapolated to $[D] = 0$, the desorption rate is estimated from eq 13 to be $k_{\text{des}} = 230 (\pm 50) \text{ s}^{-1}$. This value of the desorption rate is comparable in magnitude to that of ANS desorbing from a alkylated silica surface under strong retention conditions.⁶ Finally, these intercept results can also be used to estimate the effective concentration of surface sites, $[S]$, that governs the adsorption rate contribution to the observed relaxation kinetics. Use of the above result for the desorption rate and a diffusion-limited value of the adsorption rate constant in eq 12 indicates that the local concentration of sites that govern these kinetics is $\sim 10 \mu\text{M}$. This value greatly exceeds the excited-state concentration (to produce pseudo-first-order kinetics) and is similar in magnitude to the local site concentration previously determined for adsorption kinetics of ANS onto an alkylated silica surface.⁶ While equilibrium isotherm results indicate a larger value for the average site concentration,⁵ the smaller kinetic result may indicate that transport of molecules to surface sites is hindered by pore geometry.

CONCLUSIONS

Adsorption of the anionic dye rose bengal to a C-18 derivatized silica surface was facilitated by addition of electrolyte to solution. The shielding of the adsorbate from the negatively charged surface by compression of the double-layer thickness to dimensions comparable to the C-18 layer allowed strong adsorption of the dye to the C-18 ligands through hydrophobic interactions. Since the dipole moment of the excited triplet state of rose bengal is greater than the ground state, photoexcitation was capable of perturbing the equilibrium between the adsorbed and free-solution molecules. Under strong adsorption conditions, a relaxation to

this perturbation could be observed as a fast rise in the phosphorescence emission of the excited probe molecule due to an increase in the number of excited dye molecules in solution. The triplet populations in free solution and on the surface are quenched by ferricyanide. The decay kinetics are homogeneous, and the observed quenching rate constants represent averages for quenching of triplets on the surface and in solution since the rapid adsorption/desorption kinetics average the decay behavior of the two populations. The magnitude of the interfacial quenching rate constants is smaller than the corresponding free-solution values, which is expected due to the lower quencher encounter rates for adsorbed dye molecules.

The time-dependent change in the concentration of triplet states in solution makes a detectable increase in the phosphorescence intensity, as modeled by an exponential rise in the phosphorescence transients. The observed relaxation rate for this population varies linearly with rose bengal concentration in response to changes in the adsorption rate from solution. The corresponding adsorption rate constant based on excited triplet rose bengal concentrations was found to be faster than a diffusion-controlled limit. Realistic values for the adsorption rate constant at the diffusion-controlled limit were obtained when the rate constant was evaluated relative to the ground-state rose bengal concentration. This result is consistent with efficient energy transfer between excited triplet and ground-state rose bengal at a C-18 silica/solution interface. While interfacial energy transfer between excited- and ground-state probe molecules is an interesting phenomenon to have observed, its influence on these results ensures that the reported adsorption/desorption rates correspond to the kinetics of the ground-state probe molecules. The locally high concentration of adsorbed probe molecules and their high interfacial mobility can make energy transfer an important process in the photophysics of excited states on surfaces. Finally, the photoexcitation dipole-jump method was shown to produce adsorption/desorption kinetics results at C-18 modified silica surfaces that are comparable to those observed using temperature-jump methods, without the requirement of an energetic Joule-discharge or laser-heating pulse to perturb the interfacial equilibrium.

ACKNOWLEDGMENT

This work was supported in part by the National Science Foundation under Grants CHE-9817534 and CHE-0137569.

Received for review July 10, 2001. Accepted March 6, 2002.

AC010772T